



Article

Uptake of Zn^{2+} and As^{3+} from Wastewater by Adsorption onto Imine Functionalized Magnetic Nanoparticles

Mike O. Ojemaye ^{1,2,*} , Omobola O. Okoh ^{1,2} and Anthony I. Okoh ² 

¹ Department of Pure and Applied Chemistry, University of Fort Hare, Alice 5700, South Africa; ookoh@ufh.ac.za

² South African Medical Research Council (SAMRC), Microbial Water Quality Monitoring Centre, University of Fort Hare, Alice 5700, South Africa; aokoh@ufh.ac.za

* Correspondence: mikeojemaye@gmail.com; Tel.: +27-603-279-482

Received: 14 September 2017; Accepted: 7 December 2017; Published: 4 January 2018

Abstract: In this paper, imine functionalized magnetic nanoparticles (MNP-Maph) were employed to aqueous solutions for the uptake of Zn(II) and As(III). Characterization of the material showed the successful synthesis of this material. Factors affecting the uptake of metal ions in aqueous solution such as change in pH, time, adsorbent dose, adsorbate concentration, and temperature were investigated and optimized to determine the best experimental conditions for the effective adsorption of Zn(II) and As(III) from wastewater samples. The adsorption capacity of MNP-Maph followed similar patterns as that of amine functionalized magnetic nanoparticles (MNP-NH₂) for the uptake of both metal ions from aqueous solution when solution pH was varied. Higher pH values favored the uptake of Zn(II) and As(III) by using both adsorbents. Also, increasing the contact time and temperature yielded a higher uptake of Zn(II) and As(III). Both processes can best be described with a pseudo-second order kinetic model, while the Langmuir maximum adsorption capacity (q_m) for Zn(II) increased from 35.83 to 54.53 mg g⁻¹, and for As(III) from 50.08 to 57.60 mg g⁻¹. Of note is that the q_m of As(III) was higher than that of Zn(II) because of the lower concentration of As(III) in solution compared to that of Zn(II), and thermodynamic parameters indicated that the adsorption processes were heat absorbing and rapid in nature. Experiments to evaluate if the adsorbent could be recycled showed excellent recyclability capacity of MNP-Maph after seven runs. Lastly, application of MNP-Maph for the uptake of Zn(II) and As(III) from municipal wastewater samples showed remarkable sorption performance confirming the potential of imine functionalized magnetic nanoparticles as an excellent adsorbent for the uptake of metal ions from aqueous solutions.

Keywords: magnetic nanoparticles; adsorption; aqueous solution; Schiff base; functionalization; zinc; arsenic

1. Introduction

Magnetic nanoparticles (MNPs) are materials with large surface-to-volume ratio and high surface energies with unique magnetic, optical, thermal, catalytic, and sorption properties, making them good candidates for advanced nanotechnological applications [1]. In order to reduce their surface energies, they undergo aggregation and a typical bare magnetic nanoparticle possesses a very high chemical activity and tends to oxidize in air, thereby causing a decrease or loss in their magnetic and dispersibility characteristics. To prevent this decrease or loss in some of their properties, there is a need to coat the surface of MNPs and effectively protect it against instability. Many of the strategies adopted for the surface modification of MNPs include covalent (such as the grafting of or surface coating with

organic molecules, including surfactants, small organic molecules, polymers and biomolecules) and non-covalent ones (such as coating with an inorganic layer, metal or non metal). Other strategies involve the grafting of other nanomaterial types onto MNPs to create composite materials. Most times, surface coating or functionalization not only stabilizes the magnetic core, but also affords further functionalization [2,3], thereby allowing the introduction of new functional groups such as -OH, -COOH, -NH₂, C=N, -NR, -SR, -F, and -Cl onto the walls or sides of the MNPs.

The use of chelating ligand, 4-[(E)-phenylmethylidene]amino}benzoic acid (Maph-COOH) for the functionalization of MNPs so as to introduce the imine functional group CH=N onto the walls of MNPs has generated huge potential in the functionalization of MNPs for environmental applications. However the application of MNPs in various research areas cannot be overemphasized because of their intrinsic properties. Despite the vast works on MNPs and their applications, more research still needs to be conducted on the functionalization of MNPs with multiple functional groups for the removal of contaminants from aqueous solution.

Bidentate chelating ligand, 4-[(E)-phenylmethylidene]amino}benzoic acid (Maph-COOH) consists of an imine functional group (-CH=N) and a terminal end -COOH group. In order to introduce imine functional groups onto the surface of MNPs, the terminal -COOH can be bonded to amine surface-modified MNPs (MNP-NH₂). Maph-COOH possesses a high capability to form bonds with metal centers through one or more of its imine groups. Even though a lot of research has been done on MNPs for the uptake of contaminants from aqueous solutions, to the best of our knowledge, no study on the functionalization of MNPs-NH₂ with Maph-COOH for the efficient removal of Zn(II) and As(III) from aqueous solutions has been reported.

Among the environmental problems today is the proliferation of heavy metals to the environment [4]. Sources of these heavy metals into the environment are mainly through the industries (such as metal plating, paint manufacturing, electric device manufacturing, mining etc.). Zinc dominance in municipal and industrial water is essential in minute quantities for the growth and development of humans. In as much as it is essential to humans, it is also very harmful to human health, especially when consumed at higher concentrations. When ingested into the body, zinc causes anemia, stunted growth, and sometimes death [5]. Similarly, arsenic is regarded as one of the most toxic heavy metals for aquatic bodies and the food chain, even at extremely low concentrations. Among the negative effects of exposure to arsenic include bladder cancer, kidney and lung issues, skin irritation, and death [6,7]. Different forms of arsenic exist, and the oxidation state of any heavy metal largely determines its toxicity, with As(III) being more toxic than any other forms of arsenic in aqueous solutions [8].

Because of the enormous treat posed by these toxic metals to the environment and human beings, it is imperative to give great attention to water treatment. Far thus, various techniques such as ion exchange [9,10], coagulation [11], membrane separation [12,13], reverse osmosis [14], chemical precipitation [15], chemical oxidation [16], and adsorption [17] have been employed for the removal of heavy metals from aqueous solutions, but due to the simplicity in its operation, cost effectiveness, efficiency, and potential to regenerate adsorbents, the adsorption technique has shown to be the most reliable technique for the removal of metal ions from aqueous solutions. Also, several adsorbents such as carbon nanotubes [18], activated carbon [19], bagasse [20], lignocelluloses [21], chitosan [22,23] etc. have been reported for the removal of toxic ions from municipal and industrial effluents, but noticeable drawbacks such as high cost, generation of secondary pollutants, difficulty of separation, and low adsorption capacity are characteristics of these materials. Functionalized magnetic nanoparticles ensure increased and enhanced adsorption capacity, aid easy separation of adsorbents from solution, and are very easy to prepare.

In this paper, we investigate the removal of Zn(II) and As(III) from aqueous solutions by adsorption onto imine functionalized magnetic nanoparticles (MNP-Maph) synthesized by the covalent bonding of 4-[(E)-phenylmethylidene]amino}benzoic acid (Maph-COOH) with amine functionalized magnetic nanoparticles (MNP-NH₂). Batch adsorption studies involving the effect of time, pH,

temperature, and adsorbent dose on the adsorption of Zn(II) and As(III) from wastewater were also investigated. Also, a recyclability study was also conducted to ascertain whether Zn(II) and As(III) could be desorbed from the adsorbent so as to minimize the discharge of secondary pollutants into the environment. Furthermore, the potential of imine-functionalized magnetic nanoparticles for the removal of Zn(II) and As(III) from municipal wastewater samples obtained from the Eastern Cape Region of South Africa was evaluated at optimized conditions.

2. Experimental

2.1. Chemicals and Materials

Nickel (II) chloride ($\text{NiCl}_2 \cdot 6\text{H}_2\text{O}$) and iron (III) chloride ($\text{FeCl}_3 \cdot 6\text{H}_2\text{O}$), absolute ethanol, 25% ammonia solution, sodium hydroxide pellets, and hydrochloric acid were purchased from Merck (Pty) Ltd., Gauteng, South Africa. Chemicals such as dicyclohexylcarbodiimide (DCC), 4-aminobenzoic acid, tetraethyl orthosilicate (TEOS) and 3-aminopropyltriethoxysilane (APTES) were purchased from Sigma Aldrich, while 4-dimethylaminopyridine (DMAP) and benzaldehyde were purchased from SAAR chem (Mumbai, India) and dimethylformamide (DMF) was purchased from BDH Limited (Poole, UK). Pure zinc metal powder and diarsenic trioxide standard solution were purchased from Industrial Analytical (Pty) Ltd., Johannesburg, South Africa. All materials purchased were of analytical grade and used without further purification. Separation of magnetic adsorbents from aqueous solution was achieved by using a bar magnet.

2.2. Synthesis of Materials

2.2.1. Synthesis of 4-[(E)-Phenylmethylidene]amino)Benzoic Acid (Maph-COOH)

Maph-COOH was synthesized using the method of Kumar et al. [24] with slight modification. 4-aminobenzoic acid in (0.020 moles, 20 mL) of a mixture of ethanol and methanol (2:8 *v/v*) was added to a solution of benzaldehyde (0.20 moles) previously dissolved in a mixture of ethanol and methanol (2:8) (20 mL). Two drops of glacial acetic acid was added to the reacting mixture and refluxed at 70 °C for 10 h, the product was allowed to cool at room temperature and left to stay overnight. The product was separated by filtration and the off white powder was recrystallized in ethanol (519.6 mg, 43%), m.pt. 190–192 °C; Infra Red (ATR) (Perkin Elmer, Midrand, South Africa), cm^{-1}) 2950, 1632, 1580, 1400, 1290, 830; ^1H NMR (Nuclear Magnetic Resonance) (400 MHz, dimethyl sulfoxide, DMSO-d_6) δ : 10.0, 8.7, 8.0, 7.6, 7.3, 6.5, 2.5 and ^{13}C NMR (400 MHz, DMSO-d_6) δ : 162.45, 155.20, 136.40, 132.20, 131.06, 130.05, 129.22, 121.86, 112.00, 40.22.

2.2.2. Synthesis of Magnetic Nanoparticles (MNPs)

Magnetic nanoparticles (NiFe_2O_4) were prepared by the co-precipitation method [25]. Solutions of $\text{FeCl}_3 \cdot 6\text{H}_2\text{O}$ and $\text{NiCl}_2 \cdot 6\text{H}_2\text{O}$ in molar ratio 2:1 were prepared and 30 mL of each solution were mixed and stirred under inert atmosphere for 30 min. Sodium hydroxide (10 M) was slowly added to the reacting mixture to take the pH of the mixture to 11. The temperature of the reaction mixture was taken up to 80 °C and this mixture was stirred for 3 h more under an inert condition. The precipitate generated was collected magnetically, washed two times with ethanol and severally with deionized water until the pH was neutral and dried overnight at 80 °C. Finally, the dried powder was calcined at 450 °C for 2 h.

2.2.3. Synthesis of Silica Coated Magnetic Nanoparticles (MNP-Si)

MNPs surface was coated with silica as follows: MNP (300 mg) was placed in a 250 mL round bottom flask and dispersed in ethanol (40 mL) by using a water bath ultrasonicator for 30 min. Furthermore, tetraethoxysilane (TEOS) (3 mL) was added to the mixture and aqueous ammonia solution was used to take the pH of the reaction to 10. This mixture was continuously stirred under

nitrogen for 9 h and refluxed at 65 °C overnight. The precipitate obtained was collected by magnetically after severally washing with water and dried for 12 h at 80 °C followed by calcinating at a temperature of 450 °C within 2 h.

2.2.4. Synthesis of Amine Functionalized Magnetic Nanoparticles (MNP-NH₂)

In brief, silica-coated MNPs (200 mg) dissolved in absolute ethanol (40 mL) were ultrasonicated for 20 min in order to obtain a homogeneous mixture. Slowly added to this mixture was APTES (2 mL) and the mixture was allowed to reflux under an inert condition at 70 °C for 10 h. The dark brown crude obtained was separated, washed severally with distilled water and dried in an oven for 2 days at 100 °C [26].

2.2.5. Synthesis of Imine Functionalized MNPs (MNP-Maph)

Functionalization of MNP-NH₂ with 4-[(E)-phenylmethylidene]amino}benzoic acid (Maph-COOH) to afford imine functionalized MNPs (MNP-Maph), a novel nanomaterial was achieved by covalent bonding of the carboxylic acid group of Maph-COOH with the amino group of MNP-NH₂ [27,28]. Maph-COOH (100 mg) previously dissolved in anhydrous DMF was stirred with DCC (100 mg) for 24 h at 20 °C. Solution of MNP-NH₂ (200 mg) in anhydrous DMF and DMAP (70 mg) was added dropwise into the mixture. The suspension was further stirred for 48 h and the product obtained was collected via magnetic means in absolute ethanol to remove DMF, and washed three times with deionized water to remove DCC residues and then oven dried for two days at 100 °C.

2.3. Adsorbate Preparation

Pure zinc metal powder (1.0 g) dissolved in nitric acid (25 mL, 5 M) and made up to 1000 mL with deionized water and diarsenic trioxide standard solution purchased from the supplier were used as stock solutions. Working solutions were prepared from the different stock solutions by correctly diluting an aliquot of the latter to obtain the desired concentrations.

2.4. Adsorption Experiment

The effect of pH, contact time, adsorbent dose, adsorbate concentration, and temperature was assessed through some batch adsorption experiments involving the sorption of Zn(II) and As(III) onto MNP-Maph. In order to determine the optimum conditions for the removal of Zn(II) and As(III) from aqueous solutions, the various experimental conditions were carefully studied.

Adsorption studies between adsorbent and Zn(II) and As(III) were investigated by agitating 100 mL polypropylene plastic vials containing working solutions of Zn(II) and As(III) (20 mL, 100 mg L⁻¹) freshly prepared daily from their stock solutions using a thermostated shaker (200 rpm) at 20 °C and an adsorbent dose (40 mg) for 24 h. Appropriate amounts of NaOH or HCl (0.1 M) were used to adjust the solutions so as to attain the desired solution pH. The adsorbent was magnetically separated from the solution after the required time interval and the concentration of metal ions in solution determined by using Thermo Fischer iCE 3500 atomic adsorption spectrophotometer (AAS) (Thermo Fischer, Berlin, Germany). The % adsorbed (adsorption efficiency) and q_e (adsorption capacity) of Zn(II) and As(III) were calculated by using Equations (1) and (2) respectively.

$$\% \text{ adsorbed} = \left(\frac{C_i - C_{eq}}{C_i} \right) \times 100 \quad (1)$$

$$q_e = \left(\frac{C_i - C_{eq}}{m} \right) \times V \quad (2)$$

C_i and C_{eq} is the initial and equilibrium Zn²⁺ and As³⁺ concentration in mg L⁻¹, q_e is the adsorption capacity in mg g⁻¹, m in mg is the mass of the adsorbent and V is the volume of the adsorbate solution used in L.

Kinetics, Isotherm and Thermodynamics Studies

Kinetic studies were conducted by agitating 20 mL 100 mg L of Zn(II) and As(III) solution with an adsorbent amount of 40 mg on a thermostated shaker at 20 °C for different time intervals ranging from 1 to 240 min. The solutions were adjusted to pH 5 and 6 for Zn(II) and As(III) respectively by using 0.1 molar HCl/NaOH. After attaining the set time, the samples were separated magnetically and the concentrations of Zn(II) and As(III) were determined by AAS. Kinetic models such as pseudo-first order, pseudo-second order, intraparticle diffusion and Elovich kinetic models [19,29,30] were used to determine the process which the experimental data obeyed. Table 1 shows the equation for each model.

Similarly, isotherm experiments were studied by using different Zn(II) and As(III) concentrations ranging from 10–100 mg L⁻¹, at a fixed pH of 5 and 6 respectively. Adsorbents dose of 40 mg were agitated with a 20 mL aliquot of Zn(II) and As(III) on a thermostated oven shaker at temperature ranges of 293, 303, 313 and 318 K for 4 h. The solutions were separated magnetically and the concentration of Zn(II) and As(III) in the filtrate determined by using AAS. The experimental adsorption data were fitted into two isotherm models; Langmuir and Freundlich models [30–32]. Table 2 shows the equations of the models. Also, thermodynamic parameters such as change in Gibbs energy (ΔG°), change in enthalpy (ΔH°), and change in entropy (ΔS°) were calculated from the data obtained from the effect of temperature.

Table 1. Kinetic models investigated for the adsorption of Zn²⁺ and As³⁺.

Kinetics Model	Equation	Parameters	References
Pseudo-first order	$\ln(q_e - q_t) = \ln q_e - \frac{k_1}{2.303} t$	q_e, k_1	[29]
Pseudo-second order	$\frac{t}{q_t} = \frac{1}{k_2 q_e^2} + \frac{1}{q_e} t$	q_e, k_2	[29]
Elovich	$q_t = \frac{1}{\beta} \ln(\alpha\beta) + \frac{1}{\beta} \ln t$	α, β	[30]
Intraparticle diffusion	$q_t = k_{id} \sqrt{t} + l$	k_{id}, l	[33]

Notes: q_t , amount of adsorbate adsorbed at time t (mg g⁻¹); q_e , amount of adsorbate adsorbed at equilibrium (mg g⁻¹); α , adsorption rate constant (mg g⁻¹ min⁻¹); β , desorption rate constant (g mg⁻¹); k_1 , pseudo-first order rate constant (min⁻¹); k_2 , pseudo-second order rate constant (g mg⁻¹ min⁻¹); k_{id} , intraparticle diffusion rate constant (mg g⁻¹ min^{0.5}); l = boundary layer thickness constant (mg g⁻¹).

Table 2. Isotherm models investigated for the adsorption of Zn²⁺ and As³⁺.

Isotherm Model	Equation	Parameters	References
Langmuir	$q_{eq} = \frac{q_m b C_{eq}}{1 + b C_{eq}}$	q_m, b	[30,31]
Freundlich	$q_{eq} = K_F C_{eq}^{\frac{1}{n}}$	n, K_F	[32]

Notes: q_{eq} = adsorption capacity (mg g⁻¹); C_{eq} = concentration of adsorbate in solution at equilibrium (mg L⁻¹); q_m = maximum monolayer capacity (mg g⁻¹); b , Langmuir isotherm constant (L mg⁻¹); K_F , Freundlich isotherm constant (mg g⁻¹) (L mg⁻¹); n = adsorption intensity.

2.5. Recyclability Studies

Recyclability studies were conducted by agitating 20 mL volume of 100 mg L⁻¹ solution of Zn(II) and As(III) and adsorbent dose of 40 mg for 6 h. The solutions were magnetically separated and Zn(II) and As(III) concentrations in solution after separation were determined. The spent adsorbents obtained after magnetic separation were dried in an oven at 100 °C for 12 h, and 30 mg of this adsorbent was agitated with 10 mL solution of a 50:50 mixture of 0.1 mol L⁻¹ HNO₃ and HCl for 1 h on a shaker at room temperature and the concentrations of Zn(II) and As(III) removed from the adsorbent were then determined by using AAS. This process was allowed to undergo seven cycles to ascertain the stability of MNP-Maph towards Zn(II) and As(III) removal from aqueous solutions.

2.6. Real Sample Analysis

At two different wastewater treatment plants in the Eastern Cape Province, five water samples were collected. Physicochemical parameters of the sampled wastewater were recorded on site and on arrival into our laboratory, the samples were processed for analysis of their initial Zn(II) and As(III) concentrations. An aliquot of 20 mL of the water samples adjusted to pH 6.7 and 6.0 for Zn(II) and As(III) respectively was agitated with 40 mg of adsorbent in polypropylene bottles at 20 °C for 60 min. After shaking by means of a thermostated orbital shaker, the solutions were magnetically separated and the final concentrations of Zn(II) and As(III) in the filtrate were analyzed. To compare the performance of the adsorbent for Zn(II) and As(III) removal in real wastewater and simulated water, a wastewater deliberately contaminated with the metal ions were also prepared and subjected to the same experimental conditions as that of the real wastewater. After adsorption, the percentage removal and adsorption capacity of Zn(II) and As(III) calculated by using Equations (1) and (2), respectively for real wastewater were compared to that of the simulated water sample.

2.7. Statistical Analysis

Linear least square regression routine in the origin software statistical computing systems was used to fit the experimental data into the kinetic and isotherm models [31]. The origin statistical software considers the adjustment of the regression coefficient square, R^2 and the minimization of the residual sum of squares (RSS). The model with the highest R^2 and the least RSS values was chosen to be adequate after a comparison of all R^2 and RSS values was done.

3. Results and Discussion

3.1. Characterization of Adsorbents

Raman spectroscopy was used to characterize imine functionalized magnetic nanoparticles so as to provide information on the surface texture of the material. This was conducted at 632.8 nm and it can be observed that (Figure 1) major peaks attributed to the presence of Maph-COOH and MNP are observed in the spectra of MNP-Maph indicating the presence of two distinct phases in the compound. For instance, the strong peak observed at 1600 cm^{-1} ascribed to C=O and C=N, and weak peaks at 1200 cm^{-1} and 1100 cm^{-1} in the spectra of MNP-Maph assigned to C-N and C-O respectively are indicative of the presence of imine ligand on the surface of magnetic nanoparticles. Similar results have also been reported by Rubim et al. (2001), and Panta and Bergmann (2015) [34,35].

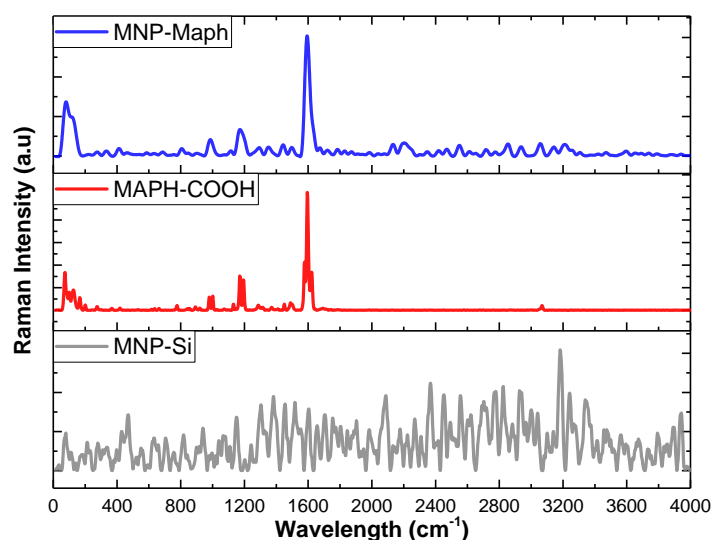


Figure 1. Raman spectra of functionalized magnetic nanoparticles.

The other characterization results of adsorbents prepared (MNP-NH₂ and MNP-Maph) have been reported in our previous work [4]. Worthy of note is the appearance of the crystalline and carbon peaks of Maph-COOH between 2 θ values of 25 and 43 in the X-ray powder diffraction (XRD) pattern of MNP-Maph, these peaks are obviously missing in the diffraction pattern of bare magnetic nanoparticles and amine functionalized magnetic nanoparticles. Also, transmission electron microscopy (TEM) images indicate that the spherical shape of MNPs was still maintained after the introduction of Maph-COOH onto MNP-NH₂. Furthermore, magnetic property measurement of MNP-Maph did not show any hysteresis and revealed that Maph-COOH incorporation onto MNP-NH₂ had little or no effect on the paramagnetic property of the azomethine functionalized magnetic nanoparticles [4].

3.2. Adsorption Experiments

The best adsorption condition for the removal of Zn(II) and As(III) from solution was determined as a function of solution pH, time, temperature, and adsorbent dose. The data were fitted into various kinetic and isotherm adsorption models so as to reveal the kind of adsorption process involved.

3.2.1. Effect of pH

Figure 2 shows the effect of solution pH on the adsorption of Zn(II) and As(III) from aqueous solutions. This was carried out over a pH range of 1–10 using MNP-NH₂ and MNP-Maph, and it is important because it determines the metal speciation and the degree of metal ionization along with the surface charge density of the adsorbent.

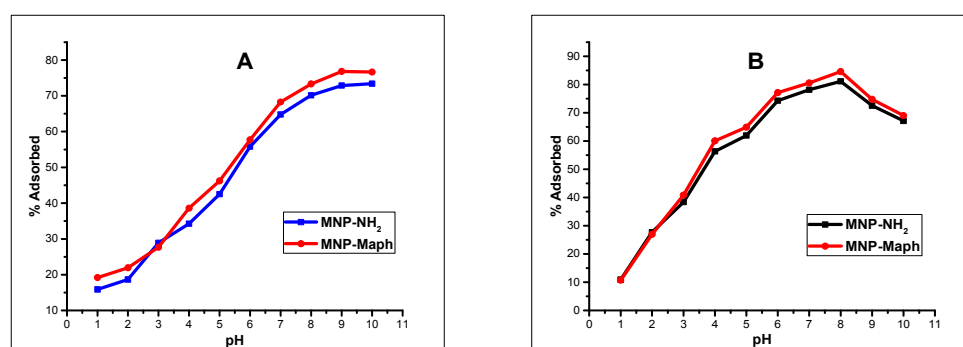


Figure 2. Effect of pH on the adsorption of (A) Zn(II) and (B) As(III) from aqueous solution by Magnetic Nanoparticle (MNP)-Maph. (conditions: 24 h contact time, adsorbent dose: 40 mg, temperature: 20 °C, adsorbate concentration: 100 mg L⁻¹, adsorbate amount: 20 mL and 200 rpm agitation speed).

Figure 2A,B shows that the uptake of Zn(II) and As(III) is pH dependent. It can be observed that at low pH values, the uptake of Zn(II) and As(III) was low as a result of the presence of other positively charged ions in solution competing for adsorption on the surface of the adsorbent. However an increase in the uptake of these ions was observed as the solution pH increases. The value of the point of zero charge, pH_{pzc} of studied azomethine-functionalized magnetic nanoparticles is 5.8 [4]. At pH values less than the pH_{pzc} , the charges on the surface of the adsorbent are positive which causes a competition for binding on the surface of the adsorbents, this result into a reduction in the removal efficiency of the adsorbent at lower pH values. At pH values greater than the pH_{pzc} , adsorption of positively charged ions is favored as a result of the small amount of positive ions at these pH values which permits ionic interaction between the adsorbent and metal ions [36]. Interestingly, MNP-NH₂ and MNP-Maph showed similar patterns in the adsorption of Zn(II) and As(III) from aqueous solution as pH increases from 1 to 10. Of note is that MNP-Maph showed greater adsorption capacity than MNP-NH₂ across all pH values. About 75% and 83% of Zn(II) and As(III) removal were obtained at pH values 10 and 8 respectively by MNP-Maph, and this could be seen to be lesser with respect to MNP-NH₂. Oyetade et al. (2017) [37] reported that most metal ions exist as precipitates at pH values

in the alkaline region, and are freely found as pure ions at pH values lower than these. Removal of metal ions by MNP-Maph occurred by ion exchange and surface complexation, with the latter taken place at higher pH values as metal hydroxides precipitates, and the former occurring at lower pH values. Two surface complexation types are known, inner and outer sphere complexations [37]. For inner sphere complexation, metal ions are chemically absorbed at the surface of the adsorbent (this is also referred to as chemisorption). Surface complexation of divalent zinc and trivalent arsenic metal ions are presented by the mechanism below (Equations (3) and (4)):



where $X = Mg^{2+}, Na^+, Ca^{2+}, K^+, Al^{3+}$ etc.

For outer sphere complexation, the interaction between metal ions and adsorbent are weaker than in the case of inner sphere complexation, and this is controlled by pH. Zinc ion uptake in the amount of 15 to 65% of the initial amount in the solution was observed between pH range 1 to 7 for MNP-Maph. When the pH increases to 8, 70% loss of zinc ion was observed and a further 78% loss was achieved at pH 10. This significant uptake of Zn(II) at pH about 7 meant that zinc hydroxide precipitation took place, and that zinc ions have been removed by hydrolysis with a K_{sp} of 1.17×10^{-17} . For As(III) removal, sorption was rapid between pH 1 to 5 from 10 to 62%. As the pH increased further from 6 to 8, a significant increase was observed, with adsorption rising to 85%. This can be ascribed to the negatively charged surface of MNP-Maph when the pH of the solution is higher than pH_{pzc} . At higher pH, precipitation of As(III) occurred as arsenic hydroxides and arsenic oxide, with the pH of precipitation theoretically at 6.2 with respect to the maximum arsenic concentration and K_{sp} ($K_{sp} = 1.38 \times 10^{-19}$). Further adsorption experiments were conducted at pH 6.7 and 6.0 for Zn(II) and As(III) respectively. Similar results for the dependence of the uptake of Zn(II) and As(III) from solution on the pH of the solution have been reported [20,38–40].

3.2.2. Effect of Time

Figure 3 shows the effect of time on the uptake of Zn(II) and As(III) from aqueous solution by MNP-Maph. Keeping the pH, adsorbent dose, agitation speed, and temperature fixed, the dependence of the adsorption of Zn(II) and As(III) from aqueous solution was assessed at three different initial divalent and trivalent ions concentrations. In Figure 3A, it can be observed that the uptake of Zn(II) was rapid within the first 10 min, and became stable just after 60 min across all initial adsorbate concentrations; this observation can be attributed to the availability of binding sites on the adsorbent within the first few minutes of subjecting the adsorbate to adsorption. Similar trends have been reported in previously conducted experiments on the uptake of Zn(II) by magnetic nanoparticles [5].

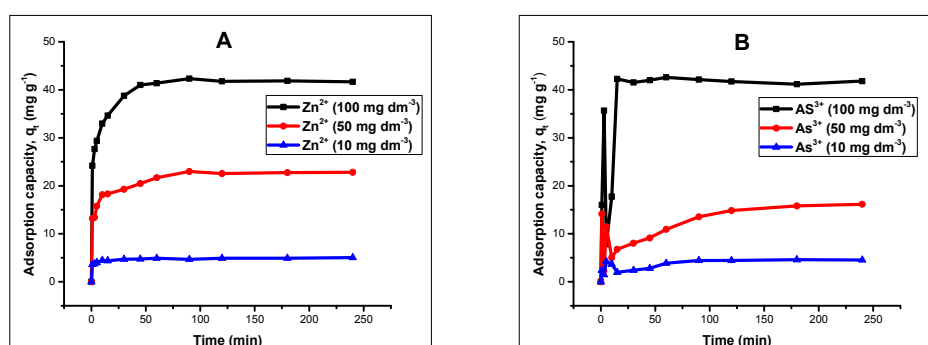


Figure 3. Effect of time on the adsorption of (A) Zn(II) and (B) As(III) from aqueous solution by MNP-Maph at pH 6.7 and 6.0 respectively (conditions: temperature: 20 °C, adsorbent dose: 40 mg, adsorbate amount: 20 mL and 200 rpm agitation speed).

In the case of As(III) (Figure 3B), adsorption showed entirely different behaviors. Adsorption-desorption was observed within the first 5 min of agitating the adsorbent and adsorbate, this is was the result of the rate of desorption of As(III) in which there was enough time for As(III) desorption and exchange of the ion with other ions. This is considered to be an important factor for the fluctuation in the adsorption efficiency. Malekpour and Khodadadi (2016) [41] reported a trend similar to the one observed for As(III) in this study. After this time, the uptake the trivalent ion was observed to be stable and at equilibrium.

Kinetic Study

This is another important parameter in wastewater treatment processes, as it helps to provide detailed knowledge of the adsorption process. The data obtained from the variation in the contact time for adsorption between MNP-Maph and heavy metals ions were fitted into kinetic models. Four different kinetic models; pseudo-first order, pseudo-second order, elovich, and intraparticle diffusion models were applied on the data from this study (Table 1). The experimental data obtained in this study for Zn(II) and As(III) best fit the pseudo-second order kinetic model going by the values obtained for the coefficient of regression, R^2 and that of the residual sum of squares (RSS) (Table 3). Table 3 shows the data for the comparison of all the four models with their R^2 values and associated residual sum of squares (RSS) and Figures S1–S4 show the curves for the comparison of all kinetic models for Zn(II) and As(III) removal from aqueous solutions.

As can be seen in Figures S1–S4, a plot of time t and t/q_t gave a good linear fit and a coefficient of regression of 0.999 and 0.903 for Zn(II) and As(III) respectively, unlike the other plots from the other models (Figures S5–S8). Also, the values obtained for the experimental q_e values (q_e (exp)) were close to the values obtained from the calculated q_e values (q_e (cal)) for pseudo second order kinetic models. Similarly, the rate constant of pseudo-second order kinetic model decreased with an increasing initial adsorbate concentration; this observation is a sharp contrast to the values obtained for other kinetic models under study. Since pseudo-second order kinetic models are most likely to explain the adsorption processes for Zn(II) and As(III) uptake, the assumption then was that the rate determining step is chemisorption and bimolecular between imine group of the adsorbent and heavy metal ions. This observation is in agreement with previously conducted studies [42].

Table 3. Kinetic parameters for the uptake of Zn(II) and As(III) from aqueous solutions by adsorption onto MNP-Maph.

Models	Zn(II)			As(III)		
	10 mg L ⁻¹	50 mg L ⁻¹	100 mg L ⁻¹	10 mg L ⁻¹	50 mg L ⁻¹	100 mg L ⁻¹
q_e (exp.) (mg g ⁻¹)	5.03	22.99	41.86	4.54	16.15	42.61
Pseudo-first order						
q_e (calc.) (mg g ⁻¹)	1.60	10.66	20.11	-	-	-
K_1 (min ⁻¹)	0.044	0.036	0.057	-	-	-
R^2	0.744	0.810	0.926	-	-	-
RSS	2.051	0.934	0.796	-	-	-
Pseudo-second order						
q_e (calc.) (mg g ⁻¹)	4.99	23.05	43.48	4.73	16.94	42.92
K_1 (min ⁻¹)	0.121	0.016	0.016	0.02	0.003	0.005
R^2	0.999	0.999	0.999	0.980	0.971	0.992
RSS	1.735	0.074	0.008	58.654	6.654	0.294
Elovich						
α (mg g ⁻¹ min ⁻²)	220907.65	1025.57	231.59	6.79	21.88	41.73
β (g mg ⁻¹ min ⁻¹)	3.746	0.491	0.275	1.743	0.559	0.153
R^2	0.911	0.951	0.933	0.532	0.364	0.601
RSS	0.206	6.354	28.368	10.532	190.570	1048.232
Intraparticle diffusion						
K_{intra} (mg g ⁻¹ min ^{-1/2})	0.414	2.032	4.061	0.217	0.785	2.175
R^2	0.456	0.626	0.666	0.516	0.506	0.432
RSS	8.667	111.972	378.877	10.891	147.970	1491.840

3.2.3. Effect of Adsorbent Dose

The effect of adsorbent dose was investigated for the removal efficiency of MNP-Maph for Zn(II) and As(III) uptake at a fixed initial metal ion concentration. The effect of MNP-Maph dose on the removal of Zn(II) and As(III) was studied by varying its amount from 10 mg to 45 mg for every 20 mL 100 mg L⁻¹ adsorbate concentrations, the results are shown in Figure 4. As the adsorbent dose increased, the percentage removal also increased in both processes. For Zn(II) uptake from aqueous solution, percentage removal increased from 15–80% as the adsorbent dose increased which is due to the availability of active sites for binding on the surface of the adsorbent which increases with increasing adsorbent dose.

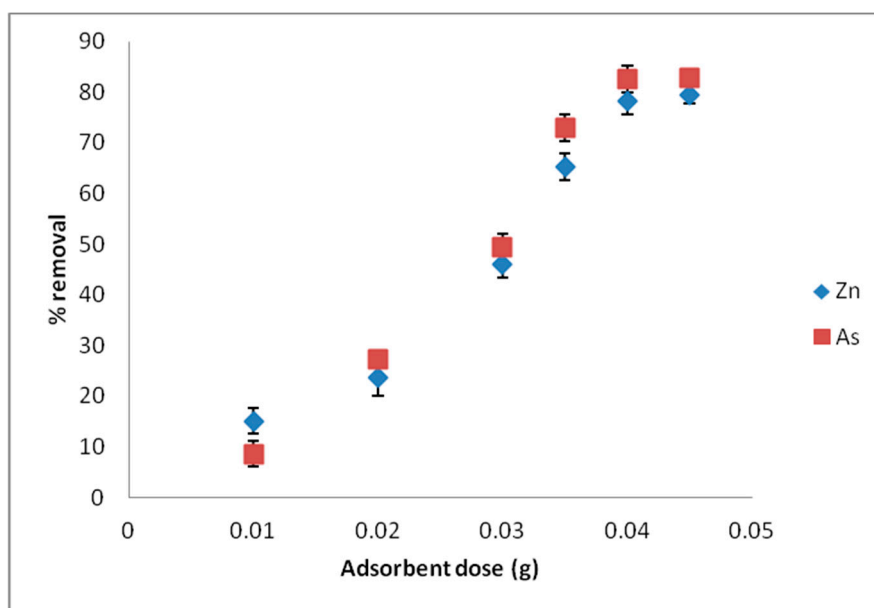


Figure 4. Effect of MNP-Maph dose on the uptake of Zn(II) and As(III) from aqueous solutions (conditions: 100 mg L⁻¹ 20 mL adsorbate solution, 20 °C temperature, 4 h contact time, 200 rpm and pH 6.7 for Zn(II), and 6.0 for As(III)).

For As(III) uptake, the removal efficiency increased with an increase in the adsorbent dose until it attained equilibrium, and As(III) uptake further showed higher percentage removal than Zn(II) demonstrating the efficiency of MNP-Maph to remove both divalent and trivalent conveniently from aqueous solutions.

Subsequent studies on the uptake of Zn(II) and As(III) were conducted by using 40 mg adsorbent dose since at this adsorbent amount; maximum uptake was noticed in both processes.

3.2.4. Effect of Temperature

The effect of temperature was carried out at four different initial adsorbate temperature between 293–318 K since temperature influences the uptake of metal ions by functionalized magnetic nanoparticles from aqueous solutions [43,44], Figure 5 indicates the influence of temperature change on the adsorption performance of MNP-Maph on the uptake of Zn(II) and As(III) from aqueous solutions. An increase in temperature resulted in an increase in the adsorption capacity of both metal ions (Figure 5A,B). This may have been as a result of an increase in the movement of metal ions in aqueous solution, and a reduction in the viscosity of the adsorbate solution at higher temperatures, favoring higher uptake of divalent and trivalent metal ions. This observation is consistent with the result obtained from previously reported studies on Zn(II), and As(III) removal from aqueous solutions [43].

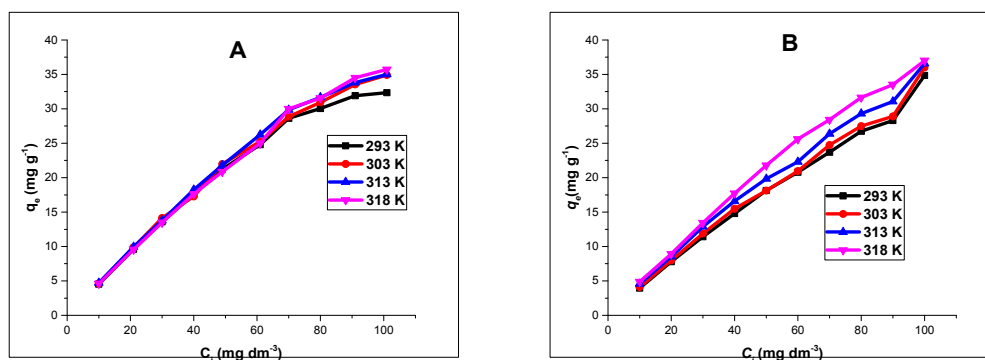


Figure 5. Effect of temperature for (A) Zn(II) and (B) As(III) uptake from aqueous solutions by MNP-Maph at pH 6.7 and 6.0 respectively (conditions: 4 h contact time, adsorbent dose: 40 mg, adsorbate amount: 20 mL and 200 rpm agitation speed).

Isotherm Study

Langmuir and Freundlich adsorption isotherm models were used to evaluate the kind of adsorption process taken place for the uptake of Zn(II) and As(III) by MNP-Maph over the temperature range of 293–318 K. The results obtained (Tables 4 and 5) showed that the data was best described by the Langmuir model than the Freundlich (Figures S9–S12), suggesting strongly that the uptake of ions on the surface for both processes is monolayer. This inference was drawn from the fact that the origin software which was used in this study for data analysis, takes into consideration the model with the lowest value of RSS , and R^2 values nearest to 1, as the model that best describes the processes. These results indicated that uptake of metal ions by MNP-Maph was a chemical type. Also, from Tables 4 and 5, data obtained showed an increase in the q_m values as temperature increased, indicating that higher temperature favors the uptake of the metal ions by MNP-Maph from aqueous solutions. Remarkably, the uptake of As(III) was observed to have a higher q_m value than Zn(II) uptake across all temperature.

When a comparison between the Langmuir maximum adsorption isotherm, q_m was done (Table 6) for the uptake of Zn(II) and As(III) between MNP-Maph and other adsorbents previously reported in literature, MNP-Maph employed in this study for the uptake of divalent and trivalent metal ions showed a better uptake of contaminants than the other adsorbents, signifying that the introduction of C=N group to the surface of MNP tremendously improved the performance of MNP as adsorbent for the removal of contaminants from wastewater. Therefore, MNP-Maph will compete favorably as an adsorbent for the removal of heavy metals from aqueous solutions.

Table 4. Isotherm parameters for the uptake of Zn(II) by adsorption onto MNP-Maph at different temperatures.

Isotherm Models and Parameter	293 K	303 K	313 K	318 K
Langmuir				
q_m (mg g ⁻¹)	35.83	39.90	39.59	54.53
b (L mg ⁻¹)	0.22	0.22	0.28	0.10
R^2	0.994	0.989	0.993	0.969
RSS	0.0042	0.0071	0.0037	0.0092
Freundlich				
K_F	7.53	7.62	7.72	7.39
N	2.06	2.02	2.02	1.96
R^2	0.897	0.908	0.908	0.923
RSS	0.333	0.306	0.305	0.266

Table 5. Isotherm parameters for the uptake of As(III) by adsorption onto MNP-Maph at different temperatures.

Isotherm Models and Parameter	293 K	303 K	313 K	318 K
Langmuir				
q_m (mg g ⁻¹)	50.08	46.71	47.17	57.60
b (L mg ⁻¹)	0.04	0.05	0.11	0.23
R^2	0.992	0.968	0.957	0.952
RSS	0.0025	0.0109	0.0151	0.0110
Freudlich				
K_F	6.29	6.50	7.14	361.28
N	0.54	0.53	0.51	0.17
R^2	0.808	0.809	0.811	0.946
RSS	0.689	0.677	0.636	50.42

Table 6. Langmuir maximum adsorption capacity, q_m for Zn(II) and As(III) uptake from aqueous solutions by MNP-Maph and other magnetic nanoparticles previously reported.

Metal Ion	Adsorbents	Conditions	q_m (mg g ⁻¹)	References
Zn(II)	Ferric hydrite coated bricks	pH 6.5, 250 mg L ⁻¹ adsorbate, 298 K, 100 mg adsorbent, 1 h.	79.5	[45]
	Magnetic amine functionalized mesoporous silica nanocomposites	pH 7.0, 20 mL 25 mg L ⁻¹ adsorbate, 298 K, 15 mg adsorbent, 5 min.	82	[46]
	Polymer modified MNPs	pH 5.5, 100 mg L ⁻¹ adsorbate, 298 K, 100 mg adsorbent, 45 min.	43.4	[47]
	Magnetic modified Chitosan	pH 5.0, 100 mg L ⁻¹ adsorbate, 298 K, 30 min.	32.16	[5]
	Microporous titanasilicate ETS-10	pH 5.0, 150 mg adsorbent, 298 K, 60 min	0.236	[48]
	MNP-Maph	pH 6.7, 20 mL 100 mg L ⁻¹ dm ⁻³ adsorbate, 293 K, 40 mg adsorbent, 4 h.	35.83	This study
	Fe ₂ O ₃	pH 7.0, room temperature, 10 mg adsorbent, 24 h.	20.0	[38]
As(III)	Fe ₃ O ₄	pH 7.0, room temperature, 10 mg adsorbent, 24 h.	5.68	[38]
	Pine leaves	pH 4.0, 298 K, 200 mg adsorbent, 35 min, 100 mL 10 mg L ⁻¹ adsorbate	3.27	[49]
	As(III)-IMHNPs	pH 6.0, 298 K, 200 mg adsorbent, 48 h, 100 mL 10 mg L ⁻¹ adsorbate.	11.52	[50]
	Carboxymethyl-β-cyclodextrin Modified MNPs	pH 9.0, 298 K, 600 mg adsorbent, 30 min, 100 mL adsorbate.	12.33	[8]
	Magnetic nickel ferrite (NiFe ₂ O ₄) MNPs	pH 9.0, 293 K, 100 mg adsorbent, 30 min, 100 mL 25 mg L ⁻¹ adsorbate.	30.86	[17]
	MNP-Maph	pH 6.0, 20 mL 100 mg L ⁻¹ adsorbate, 293 K, 40 mg adsorbent, 4 h.	50.08	This study

Thermodynamic Study

The consideration of energy and entropy in any adsorption process is important for determining whether the process will be spontaneous or not. As a result, thermodynamic parameters are significant for the application of this material and process to real life scenarios. Equations (5) and (6) were used to calculate the change in free energy ΔG° , change in enthalpy ΔH° , and change in entropy ΔS° which the adsorption processes will follow.

$$\Delta G^\circ = -RT \ln K \quad (5)$$

$$\ln k = -\frac{\Delta G^\circ}{RT} = -\frac{\Delta H^\circ}{RT} + \frac{\Delta S^\circ}{R} \quad (6)$$

where R is the gas constant ($8.314 \text{ J mol}^{-1} \text{ K}^{-1}$), T is the absolute temperature in Kelvin (K), q_e/C_e is the equilibrium constant at various temperatures, and ΔS° and ΔH° are the intercept and slope of the plot of $\ln k$ vs. $1/T$. From the data obtained from the experiment for the isotherms of the adsorption processes, we deduced the values of ΔG° , ΔH° and ΔS° (Tables 7 and 8).

Table 7. Thermodynamic parameters for Zn(II) uptake by MNP-Maph.

ΔH° (KJ mol ⁻¹)	ΔS° (J mol ⁻¹ K ⁻¹)	ΔG° (KJ mol ⁻¹)			
		293 K	303 K	313 K	318 K
0.105	3.612	-1.271	-1.479	-8.509	-8.696

Table 8. Thermodynamic parameters for As(III) uptake by MNP-Maph.

ΔH° (KJ mol ⁻¹)	ΔS° (J mol ⁻¹ K ⁻¹)	ΔG° (KJ mol ⁻¹)			
		293 K	303 K	313 K	318 K
2.417	8.258	-0.182	-0.504	-1.097	-2.066

From Tables 7 and 8, it can be observed that ΔG° values are negative across all temperature range. This confirms that both adsorption processes were spontaneous and feasible, and the fact that as the temperature increases, ΔG° values decreases, is an indication that uptake of Zn(II) and As(III) was favored at high temperatures. For a system to be endothermic in nature, ΔH° values must be positive. In both processes, ΔH° values were observed to be positive, which indicates that the processes were endothermic in nature. Also, positive ΔS° values suggested that the adsorption processes randomly increased. These processes can be considered to be physico-chemical and random, considering the results obtained for ΔG° and ΔH° , which are neither within the values specified for physisorptions nor chemisorptions only. For a physisorption adsorption process, ΔG° and ΔH° values must be in the range of 20 and 0 KJ mol⁻¹, and 21 and 20.9 KJ mol⁻¹ respectively, and for a chemisorption adsorption process, ΔG° and ΔH° values should be within -80 and -400 KJ mol⁻¹, and 80 and 200 KJ mol⁻¹ [18,30].

3.3. Regenerability Study

In order to prevent the discharge of secondary pollutants to the environment and reduce costs by making adsorbents available for reuse, regenerability studies are important to determine whether the used adsorbent can be recycled for further use, as an excellent material for adsorption should possess a good regenerability capability. A regenerability study was carried out as reported in our previous study [4], but in this case, Zn(II) and As(III) were desorbed from solution. The results indicated that an average of about 89% desorption and adsorption efficiency of Zn(II) and As(III) from aqueous solutions after seven cycles was obtained (Figure 6A,B). Hence, sorbent material possesses remarkable regenerability performance and will complement the good adsorption efficiency earlier observed with this material for the uptake of Zn(II) and As(III) from aqueous solution.

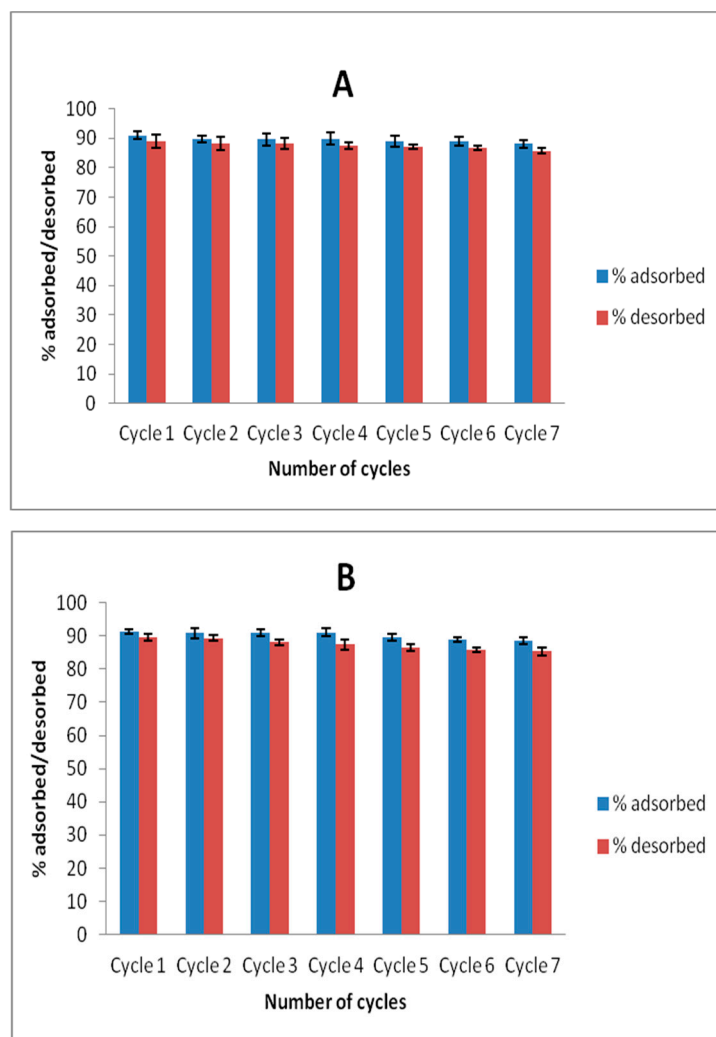


Figure 6. % adsorption and desorption for (A) Zn(II) and (B) As(III) after seven cycles.

3.4. Real Sample Analysis

For application of MNP-Maph to real wastewater, six different samples from two different wastewater treatment plants in East London area of the Eastern Cape Province were analyzed by using flame ionization atomic adsorption spectrophotometer for their initial Zn(II) and As(III) concentrations. The solution pH value was 6.0, and as a result, precipitation of Zn(II) and As(III) emerges above this pH value for both metal ions, as observed in Section 3.2.1. The other conditions of adsorption of metal ions were presented alongside the results of analysis in Tables 9 and 10. Although, the initial As(III) concentration in the real wastewater samples was found to be within 1 mg L^{-1} and Zn(II) concentration within 10 mg L^{-1} , the As(III) sample was spiked to 10 mg L^{-1} prior to adsorption experiments to enable enough As(III) ion for competition with other metal ions in solution. As a way of comparison, the real wastewater samples were subjected to adsorption studies, along with wastewater samples polluted with metal ions in the laboratory (simulated water) with similar initial metal ions concentration under equilibrium conditions using MNP-Maph. An average adsorption efficiency of 80% and 90% in the real wastewater samples and 86% and 92% in the simulated water was obtained for Zn(II) and As(III) respectively (Tables 9 and 10). The relatively low adsorption efficiency for both metal ions in the real wastewater samples can be ascribed to the complexity of the matrix [37,51]. The co-existing of other ions and organic compounds competing for active sites on MNP-Maph with Zn(II) and As(III) may lead to a decrease in their uptake performance. Nevertheless, the effect of these

interfering ions was not obvious and was negligible, demonstrating the effectiveness of MNP-Maph and the method of adsorption to selectively and sequentially remove divalent and trivalent ions from domestic and industrial wastewater. Therefore, the use of MNP-Maph for the uptake of toxic metal ions from wastewater and industrial effluents should be further considered.

Table 9. Analytical data for real wastewater samples at pH 6.0, 200 rpm, 20 °C, 0.040 g of adsorbent, 20 cm³ of adsorbate for 4 h for Zn(II).

Wastewater Treatment Plants	C_i (mg dm ⁻³)	C_{eq} (mg dm ⁻³)	Mass (g)	Volume (dm ³)	% Adsorbed (%)	q_e (mg g ⁻¹)
Simulated water Adelaide	10.88	1.52	0.0400	0.02	86.03	4.68
Influent	11.04	2.20	0.0400	0.02	80.07	4.42
After Aeration	10.89	2.14	0.0408	0.02	80.35	4.29
Effluent	9.84	1.90	0.0398	0.02	80.69	5.33
Seymour						
Influent	10.17	2.00	0.0400	0.02	80.33	4.09
After Aeration	10.11	1.92	0.0403	0.02	81.01	4.03
Effluent	10.02	1.99	0.0406	0.02	80.14	3.96

Table 10. Analytical data for real wastewater samples at pH 6.0, 200 rpm, 20 °C, 0.040 g of adsorbent, 20 cm³ of adsorbate for 4 h for As(III).

Wastewater Treatment Plants	C_i (mg dm ⁻³)	C_{eq} (mg dm ⁻³)	Mass (g)	Volume (dm ³)	% Adsorbed (%)	q_e (mg g ⁻¹)
Simulated water Adelaide	10.02	0.77	0.0402	0.02	92.30	4.60
Influent	10.50	0.98	0.0407	0.02	90.66	4.68
After Aeration	10.81	1.04	0.0402	0.02	90.38	4.86
Effluent	10.49	1.13	0.0400	0.02	89.22	4.68
Seymour						
Influent	10.32	0.86	0.0401	0.02	91.67	4.72
After Aeration	10.08	0.93	0.0408	0.02	90.77	4.49
Effluent	9.87	0.91	0.0401	0.02	90.78	4.47

4. Conclusions

Functionalized magnetic nanoparticles obtained via the covalent coupling of an imine ligand, 4-[(E)-phenylmethylidene]amino]benzoic acid (Maph-COOH) with amine modified magnetic nanoparticles (MNP-NH₂) was applied for the uptake of Zn(II) and As(III) from aqueous solutions through some batch adsorption experiments.

Characterization techniques including Raman spectroscopy showed the introduction of imine groups to the surface of magnetic nanoparticles, confirming the successful functionalization of magnetic nanoparticles with imine.

Batch adsorption experiments revealed that the processes were influenced by the pH of the solutions, contact time, and adsorbent dose. Changes in solution pH showed that higher uptake was favored at alkaline pH, and the effect of time indicated that in the first few minutes of contact between adsorbent and adsorbate solutions, there existed a sharp increase in the percentage adsorption in both divalent and trivalent ion solutions, until equilibrium was attained and the processes obeyed a pseudo-second order rate kinetic model. The Langmuir adsorption isotherm model was observed to be the most suitable isotherm model for the spontaneous processes.

Although, the uptake of As(III) was observed to be higher than that of Zn(II) in this study, the adsorbent still proved efficient for the removal of both metal ions from aqueous solutions, going by their considerably high adsorption capacity compared to that observed from previously reported studies on these contaminants. Application of this adsorbent to real wastewater samples for the uptake of Zn(II) and As(III) showed a remarkable sorption of the metal ions from aqueous

solution, indicating the capability of this material to selectively remove metal ions from a complex matrix. We therefore infer that imine-functionalized magnetic nanoparticles (MNP-Maph) are a good contender as a potential adsorbent for the uptake of Zn(II) and As(III) from aqueous solutions without separation difficulty.

Supplementary Materials: The following are available online at www.mdpi.com/2073-4441/10/1/36/s1.

Acknowledgments: We are grateful to the South Africa Medical Research Council (Grant number: MRC-RFA-GSAD-02-2014-UFH) and Govan Mbeki Research and Development Centre, University of Fort Hare for financial support.

Author Contributions: Ojemaye M.O. and Okoh O.O. conceived and planned the experiment; Ojemaye M.O. performed the experiment, analyzed the data and wrote the draft manuscript, Okoh O.O. provided reagents/materials/analysis tools and Okoh A.I. reviewed and designed the structure of the manuscript and provided part-funding for this research.

Conflicts of Interest: The authors declare no conflict of interest.

References

1. Machala, L.; Zboril, R.; Gedanken, A. Amorphous iron(III) oxide—A review. *J. Phys. Chem. B* **2007**, *111*, 4003–4018. [[CrossRef](#)] [[PubMed](#)]
2. Mahdavi, M.; Ahmad, M.B.; Haron, M.J.; Namvar, F.; Nadi, B.; Rahman, M.Z.A.; Amin, J. Synthesis, surface modification and characterization of biocompatible magnetic iron oxide nanoparticles for biomedical applications. *Molecules* **2013**, *18*, 7533–7548. [[CrossRef](#)] [[PubMed](#)]
3. Wu, W.; He, Q.; Jiang, C. Magnetic iron oxide nanoparticles: Synthesis and surface functionalization strategies. *Nanoscale Res. Lett.* **2008**, *3*, 397–415. [[CrossRef](#)] [[PubMed](#)]
4. Ojemaye, M.O.; Okoh, O.O.; Okoh, A.I. Adsorption of Cu²⁺ from aqueous solution by a novel material; azomethine functionalized magnetic nanoparticles. *Sep. Purif. Technol.* **2017**, *183*, 204–215. [[CrossRef](#)]
5. Fan, L.; Luo, C.; Lv, Z.; Lu, F.; Qiu, H. Preparation of magnetic modified chitosan and adsorption of Zn²⁺ from aqueous solutions. *Colloids Surf. B Biointerfaces* **2011**, *88*, 574–581. [[CrossRef](#)] [[PubMed](#)]
6. Alizadeh, T.; Rashedi, M. Synthesis of nano-sized arsenic-imprinted polymer and its use as As³⁺ selective ionophore in a potentiometric membrane electrode: Part 1. *Anal. Chim. Acta* **2014**, *843*, 7–17. [[CrossRef](#)] [[PubMed](#)]
7. Mu, E.; Palmero, S. Analysis and speciation of arsenic by stripping potentiometry: A review. *Talanta* **2005**, *65*, 613–620.
8. Zeinali, S.; Abdollahi, M.; Sabbaghi, S. Carboxymethyl- β -cyclodextrin Modified Magnetic Nanoparticles for effective removal of Arsenic from drinking water: Synthesis and Adsorption studies. *J. Water Environ. Nanotechnol.* **2016**, *1*, 104–115.
9. Kim, J.; Benjamin, M.M. Modeling a novel ion exchange process for arsenic and nitrate removal. *Water Res.* **2004**, *38*, 2053–2062. [[CrossRef](#)] [[PubMed](#)]
10. Volodina, E.; Pismenskaya, N.; Nikonenko, V.; Larchet, C.; Pourcelly, G. Ion transfer across ion-exchange membranes with homogeneous and heterogeneous surfaces. *J. Colloid Interface Sci.* **2005**, *285*, 247–258. [[CrossRef](#)] [[PubMed](#)]
11. Agbaba, J.; Tubic, A.; Mitic, M.; Klačnjak, M. Removal of arsenic from ground water rich in natural organic matter (NOM) by continuous electrocoagulation/flocculation (ECF). *Sep. Purif. Technol.* **2014**, *136*, 150–156.
12. Visvanathan, C.; Aim, R.B.; Parameshwaran, K. Technology membrane separation bioreactors for wastewater treatment. *Environ. Sci. Technol.* **2000**, *30*, 1–48. [[CrossRef](#)]
13. Muro, C.; Riera, F.; Díaz, C. Membrane Separation Process in Wastewater Treatment of Food Industry. *InTech* **2012**. [[CrossRef](#)]
14. Greenlee, L.F.; Lawler, D.F.; Freeman, B.D.; Marrot, B.; Moulin, P.; Ce, P. Reverse osmosis desalination: Water sources, technology and today's challenges. *Water Res.* **2009**, *43*, 2317–2348. [[CrossRef](#)] [[PubMed](#)]
15. Barakat, M.A. New trends in removing heavy metals from industrial wastewater. *Arab. J. Chem.* **2011**, *4*, 361–377. [[CrossRef](#)]
16. Ojemaye, M.O.; Okoh, O.O.; Okoh, A.I. Performance of NiFe₂O₄-SiO₂-TiO₂ magnetic photocatalyst for the effective photocatalytic reduction of Cr(VI) in aqueous solutions. *J. Nanomater.* **2017**, *2017*, 5264910. [[CrossRef](#)]

17. Karakaş, Z.K.; Boncukcuoğlu, R.; Karakaş, I.H. Adsorptive properties of As(III) from aqueous solution using magnetic nickel ferrite (NiFe_2O_4) nanoparticles: Isotherm and kinetic studies. *Sep. Sci. Technol.* **2017**, *6395*, 20–34.
18. Veličković, Z.S.; Bajić, Z.J.; Ristić, M.D.; Djokić, V.R.; Marinković, A.D.; Uskoković, P.S.; Vuruna, M.M. Modification of multi-wall carbon nanotubes for the removal of cadmium, lead and arsenic from wastewater. *Digest J. Nanomater. Biostruct.* **2013**, *8*, 501–511.
19. Ho, Y.S. Review of second-order models for adsorption systems. *J. Hazard. Mater.* **2006**, *136*, 681–689. [[CrossRef](#)] [[PubMed](#)]
20. Hamza, I.A.A.; Martincigh, B.S.; Ngila, J.C.; Nyamori, V.O. Adsorption studies of aqueous Pb(II) onto a sugarcane bagasse/multi-walled carbon nanotube composite. *Phys. Chem. Earth* **2013**, *66*, 157–166. [[CrossRef](#)]
21. Bunhu, T.; Tichagwa, L. Adsorption of methyl orange, Pb^{2+} and Cd^{2+} from aqueous solution by composites of lignocellulose-montmorillonite modified with methacryloxypropyl trimethoxysilane. *Macromol. Symp.* **2012**, *313–314*, 146–156. [[CrossRef](#)]
22. Caner, N.; Sari, A.; Tüzen, M. Adsorption characteristics of mercury (II) ions from aqueous solution onto chitosan-coated diatomite. *Ind. Eng. Chem. Res.* **2015**, *54*, 7524–7533. [[CrossRef](#)]
23. Kyzas, G.Z.; Deliyanni, E.A. Mercury (II) removal with modified magnetic chitosan adsorbents. *Molecules* **2013**, *18*, 6193–6214. [[CrossRef](#)] [[PubMed](#)]
24. Kumar, N.D.; Jha, A.; Yashmeen, S. An innovative green synthesis of some schiff bases and their antimicrobial activity. *Int. J. Pharma Bio Sci.* **2013**, *4*, 197–204.
25. Maaz, K.; Mumtaz, A.; Hasanain, S.K.; Ceylan, A.J. Synthesis and magnetic properties of cobalt ferrite (CoFe_2O_4) nanoparticles prepared by wet chemical route. *Magn. Magn. Mater.* **2007**, *308*, 289–295. [[CrossRef](#)]
26. Melnyk, I.V.; Gdula, K.; Dąbrowski, A.; Zub, Y.L. Magneto-sensitive adsorbents modified by functional nitrogen containing groups. *Nanoscale Res. Lett.* **2016**, *11*, 61. [[CrossRef](#)] [[PubMed](#)]
27. Huang, S.H.; Chen, D.H. Rapid removal of heavy metal cation and anions from aqueous solutions by an amino-functionalized magnetic nano-adsorbent. *J. Hazard. Mater.* **2016**, *163*, 174–179. [[CrossRef](#)] [[PubMed](#)]
28. Bolley, J.; Guenin, E.; Lievre, N.; Lecouvey, M.; Soussan, M.; Lalatonne, Y.; Motte, L. Carbodiimide versus click chemistry for nanoparticle surface functionalization: A comparative study for the elaboration of multimodal superparamagnetic nanoparticles targeting $\alpha\text{v}\beta 3$ integrins. *Langmuir* **2013**, *29*, 14639–14647. [[CrossRef](#)] [[PubMed](#)]
29. Fuente-Cuesta, A.; Diamantopoulou, I.R.; Lopez-Anton, M.A.; Diaz-Somoano, M.; Martínez-Tarazona, M.R.; Sakellaropoulos, G.P. Study of mercury adsorption by low-cost sorbents using kinetic modeling. *Ind. Eng. Chem. Res.* **2015**, *54*, 5572–5579. [[CrossRef](#)]
30. Liu, Y.; Liu, Y.J. Biosorption isotherms, kinetics and thermodynamics. *Sep. Purif. Technol.* **2008**, *61*, 229–242. [[CrossRef](#)]
31. Zolgharnein, J.; Shahmoradi, A. Characterization of sorption isotherms, kinetics models and multivariate approach for optimization of Hg(II) adsorption onto fraxinus tree leaves. *J. Chem. Eng. Data* **2010**, *55*, 5040–5049. [[CrossRef](#)]
32. Auffan, M.; Rose, J.; Proux, O.; Borschneck, D.; Masion, A.; Chaurand, P.; Hazemann, J.L.; Chaneac, C.; Jolivet, J.P.; Wiesner, M.R.; et al. Enhanced adsorption of arsenic onto maghemite nanoparticles: As(III) as a probe of the surface structure and heterogeneity. *Langmuir* **2008**, *24*, 3215–3222. [[CrossRef](#)] [[PubMed](#)]
33. Ho, Y.S.; McKay, G. The kinetics of sorption of divalent metal ions onto sphagnum moss peat. *Water Res.* **2000**, *34*, 735–742. [[CrossRef](#)]
34. Rubim, J.C.; Sousa, M.H.; Silva, J.C.O.; Tourinho, F.A. Raman spectroscopy as a powerful technique in the characterization of ferrofluids. *Braz. J. Phys.* **2001**, *31*, 402–408. [[CrossRef](#)]
35. Penta, P.C.; Bergmann, C.P. Raman spectroscopy of iron oxide nanoparticles (Fe_3O_4). In Proceedings of the 4th International Conference and Exhibition on Materials Science & Engineering, Orlando, FL, USA, 14–16 September 2015.
36. Lin, L.; Xu, X.; Papelis, C.; Cath, T.Y.; Xu, P. Sorption of metals and metalloids from reverse osmosis concentrate on drinking water treatment solids. *Sep. Purif. Technol.* **2014**, *134*, 37–45. [[CrossRef](#)]
37. Franus, M.; Bandura, L. Sorption of heavy metal ions from aqueous solution by glauconite. *Fresenius Environ. Bull.* **2014**, *23*, 825–839.

38. Luther, S.; Borgfeld, N.; Kim, J.; Parsons, J.G. Removal of arsenic from aqueous solution: A study of the effects of pH and interfering ions using iron oxide nanomaterials. *Microchem. J.* **2012**, *101*, 30–36. [[CrossRef](#)]
39. Fakour, H.; Lin, T. Effect of humic acid on as redox transformation and kinetic adsorption onto iron oxide based adsorbent (IBA). *Environ. Res. Public Health* **2014**, *11*, 10710–10736. [[CrossRef](#)] [[PubMed](#)]
40. Oyetade, O.A.; Skelton, A.A.; Nyamori, V.O.; Jonnalagadda, S.B.; Martincigh, B.S. Experimental and DFT studies on the selective adsorption of Pb^{2+} and Zn^{2+} from aqueous solution by nitrogen-functionalized multiwalled carbon nanotubes. *Sep. Purif. Technol.* **2017**, *188*, 174–187. [[CrossRef](#)]
41. Malekpour, A.; Khodadadi, M. Albumin-functionalized magnetic nanoparticles as an efficient sorbent for removal of Pb(II), Cd(II), Cu(II) and Cr(II) ions from aqueous solutions. *RSC Adv.* **2016**, *6*, 14705–14711. [[CrossRef](#)]
42. Chen, B.; Zhao, X.; Liu, Y.; Xu, B.; Pan, X. Highly stable and covalently functionalized magnetic nanoparticles by polyethyleneimine for Cr(VI) adsorption in aqueous solution. *RSC Adv.* **2015**, *5*, 1398–1405. [[CrossRef](#)]
43. Khan, T.A.; Dahiya, S.; Ali, I. Use of kaolinite as adsorbent: Equilibrium, dynamics and thermodynamic studies on the adsorption of rhodamine B from aqueous solution. *Appl. Clay Sci.* **2012**, *69*, 58–66. [[CrossRef](#)]
44. Lin, L.; Xu, X.; Papelis, C.; Xu, P. Innovative use of drinking water treatment solids for heavy metals removal from desalination concentrate: Synergistic effect of salts and natural organic matter. *Chem. Eng. Res. Des.* **2017**, *120*, 231–239. [[CrossRef](#)]
45. Allahdin, O.; Wartel, M.; Mabingui, J.; Boughriet, J. Kinetics of divalent metals (Cd^{2+} , Cu^{2+} , Pb^{2+} , Zn^{2+}) adsorption onto a modified brick. *Am. Chem. Sci. J.* **2014**, *4*, 687–705. [[CrossRef](#)]
46. Mehdinia, A.; Shegefti, S.; Shemirani, F. Removal of lead(II), copper(II) and Zinc(II) ions from aqueous solutions using magnetic amine-functionalized mesoporous silica nanocomposites. *J. Braz. Chem. Soc.* **2015**, *26*, 2249–2257.
47. Ge, F.; Li, M.; Ye, H.; Zhao, B. Effective removal of heavy metal ions Cd^{2+} , Zn^{2+} , Pb^{2+} , Cu^{2+} from aqueous solution by polymer-modified magnetic nanoparticles. *J. Hazard. Mater.* **2012**, *211–212*, 366–372. [[CrossRef](#)] [[PubMed](#)]
48. Lv, L.; Tsoi, G.; Zhao, X.S. Uptake equilibria and mechanisms of heavy metal ions on microporous tritanosilicate ETS-10. *Ind. Eng. Chem. Res.* **2004**, *43*, 7900–7906. [[CrossRef](#)]
49. Shafique, U.; Ijaz, A.; Salman, M.; Jamil, N.; Rehman, R.; Javaid, A. Removal of arsenic from water using pine leaves. *J. Taiwan Inst. Chem. Eng.* **2012**, *43*, 256–263. [[CrossRef](#)]
50. Song, X.; Li, L.; Geng, Z.; Zhou, L.; Ji, L. Effective and selective adsorption of As(III) via imprinted magnetic Fe_3O_4 /HTCC composite nanoparticles. *J. Environ. Chem. Eng.* **2017**, *5*, 16–25. [[CrossRef](#)]
51. Oyetade, O.A.; Nyamori, V.O.; Martincigh, B.S.; Jonnalagadda, S.B. Nitrogen functionalized carbon nanotubes as a novel adsorbent for the removal of Cu(II) from aqueous solution. *RSC Adv.* **2016**, *6*, 2731–2745. [[CrossRef](#)]

